JOURNAL OF AEROSPACE COMPUTING, INFORMATION, AND COMMUNICATION
Vol. 4, July 2007

Uncertainty Quantification in Conceptual Design via an Advanced Monte Carlo Method

Daniel P. Thunnissen*
Space Systems/Loral, Palo Alto, California 94303

Siu Kui Au†
City University of Hong Kong, Hong Kong, People's Republic of China

and

Edward R. Swenka‡
Jet Propulsion Laboratory, California Institute of Technology, Pasadena, California 91109

A method for quantifying uncertainty in conceptual-level design via a computationally-efficient probabilistic method is described. As an example application, the investigated method is applied to estimating the propellant mass required by a spacecraft to perform attitude control. The variables of the design are first classified and assigned appropriate probability density functions. To characterize the attitude control system a slightly-modified version of Subset Simulation, an efficient simulation technique originally developed for reliability analysis of civil engineering structures, is used. The proposal distribution aspect of Subset Simulation is modified vis-à-vis the original technique to account for the general characteristics of the variables involved in conceptual-level design. The results of Subset Simulation are compared with traditional Monte Carlo simulation. The investigated method allows uncertainty in the propellant required to be quantified based on the risk tolerance of the decision maker. For the attitude control example presented, Subset Simulation successfully replicated Monte Carlo simulation results yet required significantly less computational effort, in particular for risk-averse decision makers.

Nomenclature

$A_{\max}$	maximum cross-sectional area
C_d	discrete custom random variable
F	failure
G	response function
J	moment of inertia
$L(\mu, \sigma)$	lognormal random variable with parameters μ and σ
m	number of Subset Simulation levels
N	number of Subset Simulation samples
N_c	number of Markov chains developed at each simulation level; $N_c = p_0 N$

Received 11 October 2006; revision received; accepted for publication 23 May 2007.

* Senior Systems Engineering Specialist, Spacecraft Systems Engineering, 3825 Fabian Way M/S G.80. Senior Member AIAA.
† Assistant Professor, Department of Building and Construction, 83 Tat Chee Avenue, Kowloon.
‡ Senior Engineer, Autonomous Systems Division, M/S: 198-B9.

N_T	number of Monte Carlo simulation samples
$N(\mu, \sigma)$	normal random variable with parameters μ and σ
P	probability
P_{MCS}	Monte Carlo simulation value of the propellant mass required
P_x	x^{th} percentile value of the propellant mass required
$\overline{p}$	confidence level probability
p^*	proposal PDF
p_{inlet}	pressure at engine inlet
p_0	conditional probability for Subset Simulation; $p_0 \in (0, 1)$
q	spacecraft surface reflectivity
R	engine moment arm
r	effective engine moment arm
T_p	propellant temperature
$U(\text{min}, \text{max})$	continuous uniform random variable with parameters *min* and *max*
$U_d(\text{min}, \text{max})$	discrete uniform random variable with parameters *min* and *max*
X	general random variable
x	percentile value
Y	random variable representation of tradable parameter y
Y^t	true value of Y
y	tradable parameter
$\Gamma(a, b)$	gamma random variable with parameters a and b
α	engine misalignment angle
γ	correlation factor
δ	coefficient of variation (COV)
Θ	random variable representation of input parameter θ
θ	input variable (parameter)
κ	distance from the center of pressure to the center of mass
μ	mean of a normal or lognormal probability distribution
ξ	specified threshold value
$\rho_i(k)$	correlation coefficient of the indicator function $I(Y(\Theta) > \xi_{i-1})$ evaluated at k Markov chain samples apart at the i-th simulation level
σ	standard deviation of a normal or lognormal probability distribution
χ	fraction used in calculating proposal PDF width
ψ	slew angle
ω	spin rate
Subscripts	
f	final desired
i	initial
j	input variable uncertainty number
xx, yy	axes orthogonal to the spin axis
zz	spin axis

I. Introduction

SPACECRAFT are complex multidisciplinary systems with a dozen or more subsystems. Attitude control is one example of such a spacecraft subsystem (discipline). All complex multidisciplinary systems including spacecraft require engineers and designers to deal with uncertainty. Uncertainty impacts the decisions engineers and managers make in how they design complex multidisciplinary systems. This impact of uncertainty in the design of a spacecraft attitude control system (ACS) is well exemplified by the total propellant required for attitude control. The propellant mass required to maintain attitude control is one of the most important parameters that the ACS estimates during conceptual design. For spacecraft with engines as the only effectors available, the propellant available for attitude

control may determine the lifetime of the spacecraft. Furthermore, improper modeling and estimation of attitude control propellant may lead to mission failure. Quantifying the uncertainty in attitude control propellant required is also important early in the design process from a multidisciplinary standpoint as another subsystem (propulsion) is required to store and distribute this additional propellant and provide the engines to effect maneuvers. Overestimating the propellant required that is subsequently never used can have a significant "ripple effect" on the total mass and cost of the spacecraft.

Uncertainty in complex multidisciplinary systems can be classified into four types: ambiguity, epistemic, aleatory, and interaction.[1] Detailed definitions and explanations of these uncertainties as well as an overview of uncertainty taxonomies in a variety of fields are provided in [1]. Table 1 provides examples for each of these uncertainty types in the field of spacecraft attitude control. Since it is arguably more important to determine the significant sources of uncertainty in preliminary design than identifying and quantifying all uncertainty sources, Table 1 also indicates whether this form of uncertainty is viewed as significant and hence, included in the subsequent analysis.

Engineering design can be mathematically formulated as

$$\boldsymbol{y} = \mathbf{G}\left(\boldsymbol{\theta}\right) \tag{1}$$

Equation (1) represents a general expression for design where a vector $\boldsymbol{\theta}$ of input parameters (variables) is mapped to a vector $\boldsymbol{y}$ of output parameters (tradable parameters) via one or more transformation (response) functions $\boldsymbol{G}$. The response function(s) may be complicated (e.g., closed-form equations, computational algorithms, "black box" functions) requiring significant expense in time and resources to calculate values. Whereas, current design methods traditionally assume these input variables are deterministic and uncertainty is evaluated *ex-post facto*, the method described in this paper follows probabilistic design techniques that quantify the uncertainty in the tradable parameters $\boldsymbol{y}$ by accounting for all the uncertainties in the $\boldsymbol{\theta}$ input variables themselves.[2] In this context, the vector $\boldsymbol{\theta}$ in Eq. (1) is replaced by $\boldsymbol{\Theta}$ that may include discrete random variables, continuous random variables, constant values, and discrete choices among options. The set of output parameters that depend on the random vector $\boldsymbol{\Theta}$ is now denoted by the capital letter $\boldsymbol{Y}$:

$$\boldsymbol{Y} = \boldsymbol{G}\left(\boldsymbol{\Theta}\right) \tag{2}$$

Probability theory is well-known to provide a rational and consistent framework for treating uncertainties and plausible reasoning.[3–5] Probabilistic methods offer a viable approach to manage uncertainties that confront a decision maker. A decision maker is one or more individuals or organizations responsible for making final decisions in a project. We use the singular in this paper although the decision maker may consist of more than one individual or organization.

The output vector of random variables $\boldsymbol{Y}$ assumes that the given response functions $\boldsymbol{G}$ are "perfect" with no uncertainty in the response functions (models). Approximation error in a given tradable parameter (dependent variable)

Table 1 Examples of different uncertainty types.

Uncertainty type	Attitude control example	Included in this paper's analysis?
Ambiguity	The pointing control must be 2° [everywhere? continuously?]	No
Epistemic		
Model	The difference between the propellant mass predicted by an analytic model and the actual flight measured total	Yes
Phenomenological	The density profile of Neptune's atmosphere	No
Behavioral		
Design	The choice between two different engines for attitude control	Yes
Requirement	The spacecraft shall be able to de-spin from 10 rpm [and this requirement later changes to 15 rpm]	Yes
Volitional	An analysis an engineer says he will perform but does not	No
Human errors	A mistake in measuring the mass of an engine	No
Aleatory	The thrust of an engine at a given pressure	Yes
Interaction	The combination of choice between two different engines and the fact that their thrust levels are not certain	Yes

can be represented as a random variable and related to the true value:[2]

$$Y^t = Y + X \tag{3}$$

A probability density function (PDF) can be determined for X if sufficient data are available to compare to the values determined by the model. Assuming the approximation error X is independent of the model prediction Y, the cumulative distribution function (CDF) of the tradable parameter can be obtained as the convolution of the CDFs of Y and X. A CDF value is selected based on the risk tolerance of the decision maker. The risk tolerance of a decision maker will manifest itself through the percentile value, $\overline{p}$, of this CDF the decision maker chooses to believe. For example, the 90, 99, and 99.9 percentiles might provide a decision maker with low-, medium-, and high-confidence estimates in the probability that a tradable parameter will not be exceeded. These three percentiles may correspond to a risk-tolerant, risk-neutral, or risk-averse decision maker, respectively. The extreme tails of a tradable parameter distribution are important in the design of many complex engineering systems. A spacecraft may need an accurate estimate of the 99, 99.9, or 99.99 percentile values for its reliability to see if it will survive long enough to complete its mission while an aircraft would like accurate estimates of the extreme tail values of its range to be certain a target or destination can be reached in an emergency situation.

Unfortunately, the traditional method for accessing such uncertainties (Monte Carlo simulation) requires a large number of samples to accurately determine extreme tail (high- or low-percentile) values which may require a prohibitive amount of time and resources to complete. Advanced Monte Carlo methods are being developed with the aim to be applicable to complex engineering systems that involves general nonlinear response and a large number of random variables.[6,7] The method described in this paper applies an innovative sampling technique known as Subset Simulation to accurately determine CDF values of interest while significantly reducing the amount of response function calculations and hence, the total computation cost. Originally developed and applied in estimating small failure probabilities in high-dimension structural-engineering applications, Subset Simulation has been modified to handle more general situations.[8–11]

The remainder of the paper summarizes the investigated method, its application to a spacecraft ACS, and discusses the results. Details of the actual spacecraft ACS model assumed are provided in [10].

II. Method Summary

The general method to evaluate the CDF of Eq. (2) begins with identifying all the tradable parameters of concern to a decision maker. With tradable parameters identified, the engineering system (response function) is formulated mathematically. This mathematical formulation may be an analytic model for each tradable parameter. Such a model might include dozens or hundreds of equations and relations. A model may be existing off-the-shelf software or a custom program for this specific system. Much analysis for ACS, particularly for non-Earth orbiting spacecraft, is mission specific and requires customized models. Determining how accurate models need to be to effectively assess uncertainty in conceptual design is a critical issue. In this work, modeling error is addressed as an additive uncertainty, see Eq. (3), whose distribution is assigned based on expert judgment.

With models and model uncertainty assessed, the input variables are classified and given a probabilistic representation. Classifying the variables into their uncertainty types is useful in understanding their respective impact on the overall design. Variables are characterized by a PDF. The PDF applied to each variable may be determined from existing data, analogy, analysis, expert opinion, or a combination of these.

To propagate the uncertainty of the input variables and assess the probabilistic characteristics of the tradable parameters, two simulation techniques, Monte Carlo simulation and Subset Simulation, are considered in this work. The former serves as a benchmark for the latter. Uncertainty in the model (approximation error) is assessed at the final step for Monte Carlo simulation. The CDF results for the model response Y obtained by the simulation techniques are probabilistically convolved with the CDF of model uncertainty X to yield final estimate of the uncertainty in each tradable parameter Y^t which can then be used by the decision maker to guide design decisions. In Subset Simulation, model uncertainty is treated at the same level as any other uncertainty via an input variable. In this paper, model uncertainty is assumed to be Gaussian with zero mean (implying unbiased prediction) and some appropriate value of variance chosen *a prioiri*.

A. Monte Carlo Simulation

Monte Carlo simulation (MCS) solves a problem by generating suitable random numbers and observing the fraction of the numbers obeying some property or properties. Monte Carlo simulation is the most established sampling technique and the benchmark for comparison by other techniques. Monte Carlo simulation involves two steps. First, N random realizations (samples) of the uncertain input variables, $\boldsymbol{\theta}$, are generated according to their specified probability distributions. In the second step the tradable parameters $\boldsymbol{y}$ are evaluated via the response function(s) $\boldsymbol{G}$ for the generated samples and recorded. The N values for each tradable parameter can be transformed to a PDF or CDF where the mean and other statistical characteristics of interest can be calculated. Hence, for N MCS samples, a set of N vectors of input variables and a set of N vectors of tradable parameters are formed.

B. Subset Simulation

Subset Simulation (SS) is an adaptive stochastic simulation procedure for efficiently computing small tail probabilities.[8,9] Originally developed for reliability analysis of civil engineering structures, SS stems from the idea that a small failure probability can be expressed as a product of larger conditional failure probabilities for some intermediate failure events, thereby converting a rare event simulation problem into a sequence of more frequent ones.

Without loss of generality, assume one tradable parameter Y and that it is positive-valued. For a specified threshold value ξ for which $P(Y > \xi)$ is of interest, let $0 < \xi_1 < \xi_2 < \cdots < \xi_m = \xi$ be an increasing sequence of intermediate threshold values. By the definition of conditional probability,

$$P(Y > \xi) = P(Y > \xi | Y > \xi_{m-1}) \cdot P(Y > \xi_{m-1}) = \cdots = P(Y > \xi_1) \prod_{i=2}^{m} P(Y > \xi_i | Y > \xi_{i-1}) \tag{4}$$

The original idea of SS is to estimate $P(Y > \xi_1)$ and $\{P(Y > \xi_i | Y > \xi_{i-1}) \colon i = 2, \ldots, m\}$ by generating samples of $\boldsymbol{\Theta}$ conditional on $\{Y(\boldsymbol{\Theta}) > \xi_i\}, i = 1, \ldots, m$. In implementations, the intermediate failure threshold values $\xi_1, \ldots, \xi_m$ are generated adaptively using information from simulated samples so that the sample estimate of $P(Y > \xi_1)$ and $\{P(Y > \xi_i | Y > \xi_{i-1}) \colon i = 2, \ldots, m\}$ always correspond to a common specified value of the conditional probability p_0. By carrying out the procedure until $\xi_m > \xi$, the simulated samples provide information for establishing the CDF of Y covering the small-tail probabilities of interest.

1. Markov Chain Monte Carlo

The efficient generation of conditional samples is pivotal in the success of SS. In general, it is highly non-trivial (if possible) to generate independent samples according to an arbitrarily given distribution but it turns out that it is possible to generate dependent samples according to the distribution. This is made possible through the machinery of Markov Chain Monte Carlo (MCMC) simulation.[12] Markov Chain Monte Carlo is a class of powerful algorithms for generating samples according to any given probability distribution. It originates from the Metropolis algorithm developed by Metropolis et al. for applications in statistical physics.[13] A major generalization of the Metropolis algorithm was due to Hastings for applications in Bayesian statistics.[14] In MCMC, successive samples are generated from a specially designed Markov chain whose limiting stationary distribution tends to the target PDF as the length of the Markov chain increases. Markov chain samples explore and gain information about the failure region as the Markov chain develops.

An essential aspect of the implementation of MCMC is the choice of 'proposal distribution' which governs the generation of the next sample from the current one. Such a choice depends on the nature of the input variables as well as the sensitivity of the failure probability to each of these parameters. The efficiency of SS is robust to the choice of the proposal distribution, but tailoring it for a particular class of problem can certainly improve efficiency. Reported results in structural reliability applications also reveal that the efficiency is also relatively insensitive to the complexity of the problem.[15,16] The computational effort, measured in terms of the number of samples required to achieve a given coefficient of variation of probability estimate, generally grows in a logarithmic fashion (specifically, as $O((\log P)^2)$ as the target probability level P decreases, in contrast to $O(1/P)$ for traditional Monte Carlo.[9]

2. Procedure Overview

The procedure for adaptively generating samples of $\boldsymbol{\Theta}$ conditional on $\{Y(\boldsymbol{\Theta}) > \xi_i\}$, $i = 1, \ldots, m$ by SS, is summarized as follows. First, N samples $\{\Theta_{0,k}: k = 1, \ldots, N\}$ are simulated by direct Monte Carlo simulation, i.e., they are independent and identically distributed (i.i.d.) as the original PDF. The subscript '0' here denotes that the samples correspond to 'conditional level 0' (i.e., unconditional). The corresponding values of the tradable variable $\{Y_{0,k}: k = 1, \ldots, N\}$ are then computed. The value of ξ_1 is chosen as the $(1 - p_0)N$-th value in the ascending list of $\{Y_{0,k}: k = 1, \ldots, N\}$, so that the sample estimate for $P(F_1) = P(Y > \xi_1)$ is always equal to p_0. Here, we have assumed that p_0 and N are chosen such that p_0N is an integer and $P(F_1)$ corresponds to the probability of being in the (first) failure region.

Due to the choice of ξ_1, there are p_0N samples among $\{\boldsymbol{\Theta}_{0,k}: k = 1, \ldots, N\}$ whose response Y lies in $F_1 = \{Y > \xi_1\}$. These are samples at 'conditional level 1' and are conditional on F_1. Starting from each of these samples, MCMC is used to simulate an additional $(1 - p_0)N$ conditional samples so that there is a total of N conditional samples at conditional level 1. The value of ξ_2 is then chosen as the $(1 - p_0)N$-th value in the ascending list of $\{Y_{1,k}: k = 1, \ldots, N\}$, and it defines $F_2 = \{Y > \xi_2\}$. Note that the sample estimate for $P(F_2|F_1) = P(Y > \xi_2|Y > \xi_1)$ is automatically equal to p_0. Again, there are p_0N samples lying in F_2. They are samples conditional on F_2 and provide "seeds" for applying MCMC to simulate an additional $(1 - p_0)N$ conditional samples so that there is a total of N conditional samples at "conditional level 2."

This procedure is repeated for higher conditional levels until the samples at 'conditional level $(m - 1)$' have been generated to yield ξ_m as the $(1 - p_0)N$-th value in the ascending list of $\{Y_{m-1,k}: k = 1, \ldots, N\}$ and that $\xi_m > \xi$ so that there are enough samples for estimating $P(Y > \xi)$. Note that the total number of samples, i.e., number of evaluations of the tradable variable, required by SS is equal to $N_T = N + (m - 1)(1 - p_0)N$. This procedure is illustrated in Fig. 1.

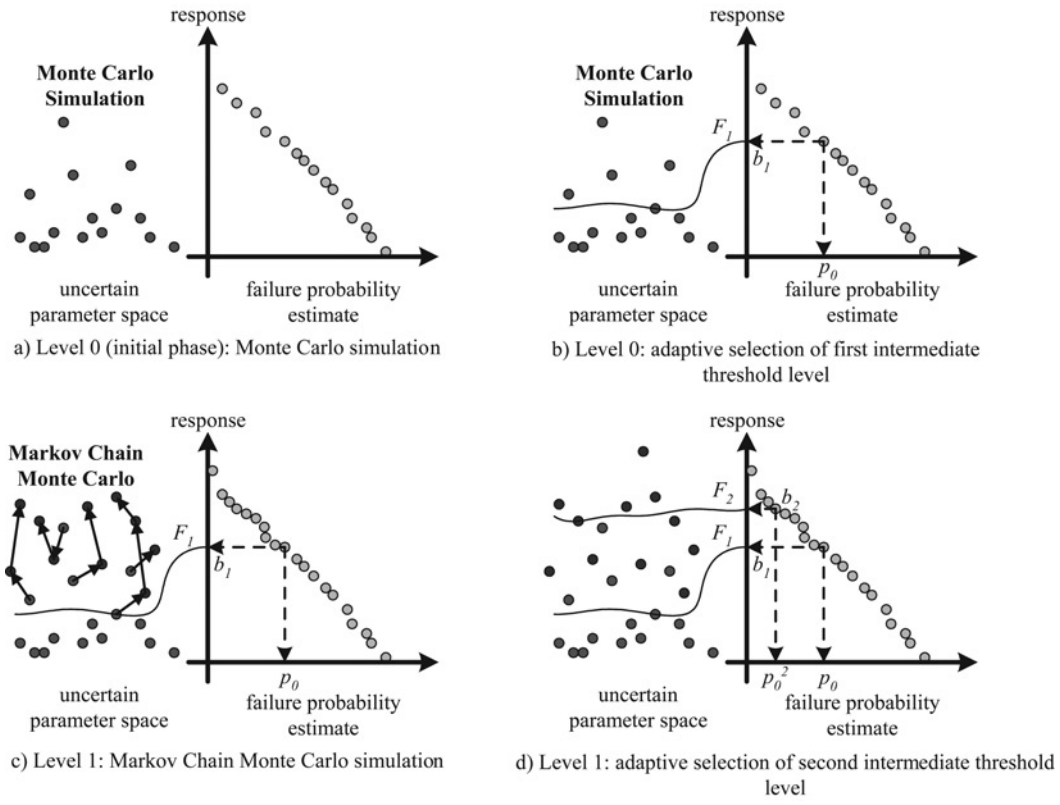

Fig. 1 Illustration of Subset Simulation procedure.

The choice of p_0 affects how fast the target probability level is reached. Clearly, a large value of p_0 leads to more samples accepted for the next simulation level but SS then requires more levels to reach the target probability level. Conversely, when p_0 is small only a small fraction of samples are accepted for the next level. In this case the target probability level may be reached faster but at the expense of a higher error in the corresponding threshold value ξ. Numerical experiments show the efficiency of SS is robust to the choice of p_0 on the range 0.1 to 0.5. For convenience in implementation, $p_0 = 0.1$ is often chosen.

3. Modifications to Algorithm

Originally developed and applied in estimating small failure probabilities in high-dimension structural-engineering applications, the SS algorithm in [8] and [9] is modified to handle more general situations such as the uncertainty in engineering design formulation provided by Eq. (2). The major modification made to the algorithm developed by [8] is in the type of input variables and their corresponding proposal PDFs (p_j^*). In [8] only continuous input variables were considered and a continuous uniform distribution centered at the current input variable value with a width equal to $2\chi\sigma_j$ was always used for the proposal PDF. The variables in the design of a complex multidisciplinary system may be continuous, discrete, and discrete choices among alternatives so additional and mathematically valid proposal PDFs are implemented as shown in Table 2.

4. Parameters of Interest

Approximate formulae have been derived to assess the error in the failure probability estimates.[9] The derivation assumed the intermediate threshold values $\xi_1, \ldots, \xi_m$ were fixed. In particular, the coefficient of variation (COV) δ of the estimate for $P(Y > \xi_m)$, defined as the ratio of its standard deviation to its mean, may be bounded above by using

$$\delta^2 \leq \sum_{i,j=1}^{m} \delta_i \delta_j + o(1/N) \tag{5}$$

where δ_i is the COV of the estimate for $P(Y > \xi_i | Y > \xi_{i-1})$ (with the convention that $P(Y > \xi_1 | Y > \xi_0) = P(Y > \xi_1)$), given by

$$\delta_i^2 = \frac{1 - p_0}{p_0 N} (1 + \gamma_i) \tag{6}$$

Table 2 Proposal PDFs for different uncertain input variables.

Input variable	Proposal PDF p_j^*	Description
Continuous	$U(\theta_k(j) - \chi\sigma_j, \theta_k(j) + \chi\sigma_j)$	a continuous uniform distribution centered at the current input variable value with a width equal to $2\chi\sigma_j$
Discrete	$U_d(\lfloor\theta_k(j) - \chi\sigma_j\rfloor, \lceil\theta_k(j) + \chi\sigma_j\rceil)$	a discrete uniform distribution centered at the current input variable value with a width equal to $2\chi\sigma_j$ rounded to the nearest integers
Discrete choice among options	$C_d(\sim)$	a discrete custom distribution that is identical to the actual variable PDF q_j when the most probable value is the current sample; otherwise the current sample and the most probable value probabilities are swapped (other PDF values and probabilities are unchanged)
Constant	n/a	unchanged for all samples in a given Markov chain so no p_j^* is needed

In Eq. (6), γ_i is a correlation factor that reflects the correlation among the samples at the $(i-1)$-th conditional level. It is given by

$$\gamma_i = 2 \sum_{k=1}^{N/N_c - 1} \left(1 - \frac{kN_c}{N}\right) \rho_i(k) \tag{7}$$

where p_0 is assumed to be chosen such that $N_c = p_0 N$ is an integer and $\rho_i(k)$ can be estimated using the simulated samples. Note that $\gamma_1 = 0$ as the initial simulation stage corresponds to a traditional MCS. The value of γ_i for $i = 2, \ldots, m$ can be estimated using the Markov chain samples at each $(i-1)$-th conditional level. Since from Eq. (6), δ_i is $O(1/\sqrt{N})$, Eq. (5) indicates that that the COV δ of the failure probability estimate is $O(1/\sqrt{N})$, which is similar to standard Monte Carlo simulation. The actual value of δ depends on the correlation between the intermediate conditional probability estimates, which arises from the fact that some of the samples from one simulation level are used for generating the samples of the next level.

It should be noted that there is a relationship between χ and γ. The scaling parameter χ specifies the spread of p_j^*. The spread governs the maximum allowable distance that the next sample in a Markov chain can depart from the current one and hence affects the size of the region that can be covered by the algorithm within a given number of steps. In general, the larger the spread, the larger the region covered by the Markov chain samples. Smaller spreads (small value of χ) tend to increase the correlation among Markov chain samples (low value of γ), slowing down the convergence of the MCMC estimator. Conversely, a large spread (high value of χ) will increase the number of repeated samples (high value of γ) and thus also slow down the convergence of the MCMC estimator. The reason for this latter situation is that when the spread is large a candidate state will often be generated far away from the current sample. A candidate state may therefore not have a high probability of lying in the "failure" region and hence be rejected frequently. Thus, the choice of the spread of p_j^* is a trade off between correlation effects arising from proximity and repeated samples from rejection.

III. Application

The investigated method is applied to estimating the propellant required for attitude control by a spacecraft, specifically the Jet Propulsion Laboratory (JPL)/NASA Mars Exploration Rover (MER) cruise stage. The analysis that follows was performed *ex-post facto* at an assumed period just before the preliminary design review (PDR). Preliminary design review is one of the most important periods for determining and updating uncertainty estimates in the development of an ACS. Although not performed in this paper, the method can be repeated at other times during design to further update uncertainty estimates. For simplicity, only one tradable parameter, namely the propellant mass required, is investigated. The results of this method are compared to the actual MER ACS values.

A. Mars Exploration Rover Spacecraft

The MER project had the primary objective of placing two mobile science laboratories, MER-A (*Spirit*) and MER-B (*Opportunity), on* the surface of Mars in order to remotely conduct geologic investigations, including characterization of a diversity of rocks and soils that may hold clues to past water activity. The MER project used the 2003 launch opportunity to deliver two identical rovers to different sites in the equatorial region of Mars. The MER project was managed by JPL, a federally funded research and development facility managed by the California Institute of Technology for NASA. The design of MER officially began in April 2000. The MER flight system was an adaptation of the Mars Pathfinder (MPF) spacecraft design which was launched in 1996 and landed successfully on Mars on 4, July 1997.

The MER flight system comprised four major components: an Earth-Mars cruise stage; an entry, descent, and landing system; a lander; and a mobile science rover with an integrated instrument package. Figure 2 illustrates the MER flight system in its Earth-Mars cruise configuration. The MER ACS was designed and developed by JPL/NASA with several contractors providing components and expertise. Except for the shared flight computer and inertial measurement units, the ACS resided on the cruise stage. The MER ACS flight software was run on the command and data handling system that resided on the rover within the lander. This was possible via a connection between the rover support board and the remote electronic unit on the cruise stage. During the interplanetary transfer from Earth to Mars, MER was a spin-stabilized spacecraft with a nominal spin rate of 2 rpm and the cruise stage

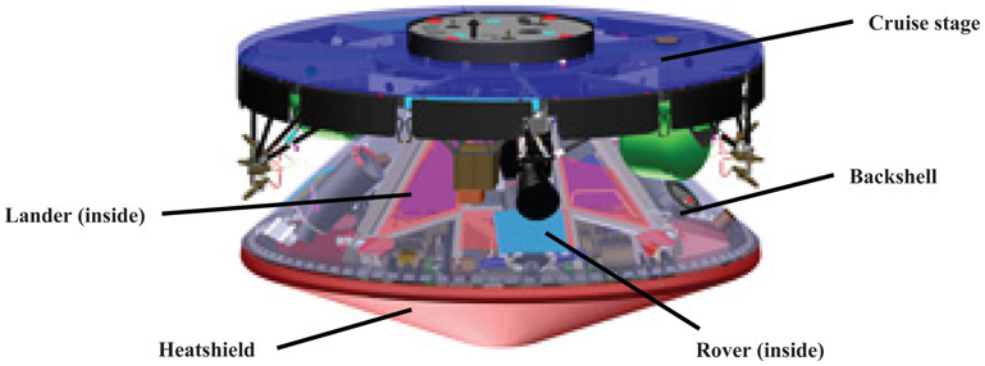

Fig. 2 MER spacecraft during cruise to Mars.

provided most of the traditional spacecraft subsystem functionality, such as propulsion, power, communications, thermal, and attitude control.[17] Roncoli and Ludwinski[17] discuss the MER mission in detail. The MER cruise stage used two clusters of four 4.5 N Aerojet MR-111C engines (thrusters), one on each side as shown in Fig. 3. The z-axis is the spin axis. The spin axis moment of inertia is the spacecraft's maximum moment of inertia. The two engine clusters are on the $+x$ and $-x$ axes. The $+y$ axis is out of the page in Fig. 3. Engines 1, 2, 5, and 6 are in the x-z plane whereas engines 3, 4, 7, and 8 are in the x-y plane. All engines are canted at an angle of 40° from the x-axis. The effective moment arm of all engines is therefore $r = R \cdot \sin 40° \approx 0.643R$. Two engines, one on each side of the spacecraft, with equal and opposite thrust vectors are fired for attitude re-orientation or slew maneuvers. Ideally, a torque is imparted only about the spacecraft's center of mass and no change in the spacecraft trajectory results. For example, firing engines 3 and 8 would spin the spacecraft (counter clockwise) about the $+z$ axis. The propellant required on MER for attitude control was estimated at 4.4 kg using a worst-case deterministic approach.[18]

B. Model Assumptions

The total propellant required by the spacecraft for attitude control is the sum of the propellant required for overcoming all spin/de-spin maneuvers, required attitude update maneuvers including any possible fault protection (safe mode) recovery maneuvers, and allocations for external disturbance (i.e., solar torque build-up) compensation. The model described in [10] is assumed for calculating these individual propellant mass maneuver values sequentially based on the time they occur from Earth launch. This model was created to analyze the MER flight system (cruise stage), specifically the Earth-to-Mars interplanetary-cruise portion of the mission. Although the model described

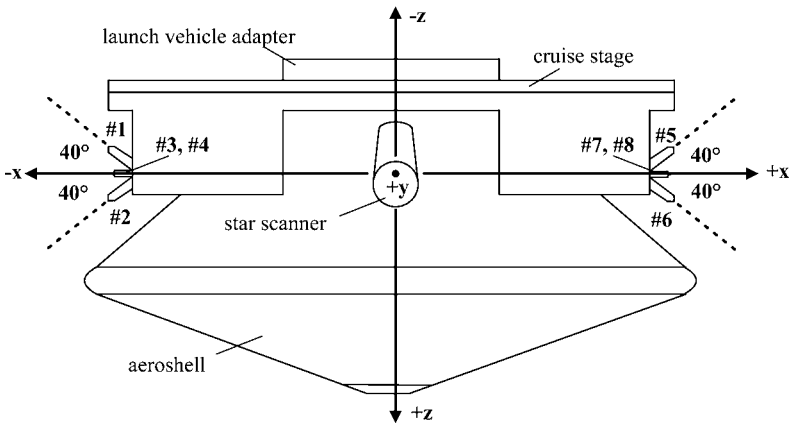

Fig. 3 MER engine cluster configuration.

in [10] is a general attitude-control model based on the re-orientation motion of a rigid spacecraft found in references [19] and [20], the application of this model and analysis to other spacecraft would require verification of the assumptions and possible alterations. The major assumption in this model and analysis is the use of a simple feedback control model. The behavior of an actual ACS system can be understood only if feedback control is correctly implemented and modeled. Nonetheless, for the conceptual estimation of propellant required for attitude control, the difference between a sophisticated feedback control model and the feedback model implemented is likely small. Higher-fidelity models implementing feedback control for all maneuvers could readily be substituted for the simple models described. Model uncertainty addresses this difference and is accounted for in the analysis. Additional model assumptions assumed are provided in [10].

C. Model Formulation

The model described in [10] actually combines three sub-models. Each of the three sub-models calculates the propellant required for spacecraft attitude control maintenance: spinning/de-spinning the spacecraft, slewing the spacecraft, and compensating for external disturbances. In total the three sub-models comprise over three dozen physics-based equations and almost 60 input variables. This propellant mass model represents the response functions $\boldsymbol{G}$ in Eqs. (1) and (2).

1. Spin/De-spin Maneuvers

Spinning a spacecraft up or down is done for a variety of reasons including instrument operation, thermal control, and cleaning-up launch vehicle dispersions. All three were the case with the MER flight system. The MER design used a Ball Aerospace CS-203 star scanner requiring a nominal spin rate of 2 rpm to successfully operate during the Earth-Mars cruise. This decision in turn impacted the thermal design.[21] Lastly, the third stage of the Boeing Delta II launch vehicle that was used to inject MER on its interplanetary trajectory was spun up to 70–80 rpm for gyroscopic stiffness against disturbances during operation of its solid rocket motor. After the solid rocket motor burned out, the spin rate was reduced to 12 rpm by the launch vehicle's yo-yo de-spin system, and reduced further to 2 rpm by the ACS for the entire cruise to Mars. As discussed earlier, a simple feedback was implemented in this model to account for uncertainties, particularly in the thrust of the engines used. The aforementioned procedure is repeated until the actual spin rate is within a specified value of the desired spin rate (assumed to be 0.2 rpm in this analysis).

2. Slew Maneuvers

Slew (Re-point) maneuvers are performed by spacecraft for thermal control, power generation, telecommunication, and observation. In the case of MER, the spinning cruise stage slewed periodically from the nominal orientation to one in which the communication antennae could be pointed correctly towards the Earth. These slews for antennae pointing, by design, also met thermal and power requirements of the spacecraft. The slew algorithm presented in [10] is complicated by the fact that only a discrete number of engine pulses is possible and that the thrust of the engines used for pulsing is uncertain. A pointing control requirement of 2° is assumed in the subsequent analysis. The simple feedback model for slewing could be replaced by a more sophisticated algorithm that determines the angle slewed after each pulse if components onboard are sophisticated enough to measure these small changes.

3. External Disturbance Compensation

The only external torque experienced by MER during its interplanetary cruise is a solar pressure torque. The sub-model presented in [10] calculates the solar torque build-up on a daily basis as well as after each other type of maneuver. When the spacecraft slews an amount greater than the pointing control requirement due to this solar torque, the spacecraft is re-oriented via a controlled slew maneuver described in the previous section. The amount of propellant required for each of these slew corrections follows the slew maneuver sub-model previously discussed.

D. Classification and Probabilistic Modeling of Variables

The input variables involved in the propellant mass model are classified as aleatory, design, or requirement uncertainties. The classification aids in understanding the impact of uncertainty in the design of the ACS. This analysis is different from similar analyses, e.g. [22] and [23], in that much of the uncertainty is in the actual operation (mission sequence) of the final subsystem and not in the design. However, these uncertainties in the operation of

Table 3 General input variables.

Variable	Type	Distribution type and parameter	Units
p_{inlet}	aleatory	$N(690, 23)$	kPa
T_p	aleatory	$N(25, 2.5)$	°C
α	aleatory	$N(0, 0.5)$	deg
q	aleatory	$N(0.6, 0.06)$	–
J_{xx}	design	$U(300, 450)$	kg-m^2
J_{yy}	design	$U(300, 450)$	kg-m^2
J_{zz}	design	$U(450, 600)$	kg-m^2
$A_{\max}$	design	$N(5.31, 0.053)$	m^2
κ	design	$U(0.6, 0.7)$	m
R	design	$N(1.3, 0.0013)$	m
g_s	aleatory	$N(1400, 14)$	W/m^2
ω_i	requirement	$N(12, 1.33)$	rpm

the final subsystem are significant and do impact the design of the subsystem. Uncertainties in the general variables are first discussed. Uncertainty in the mission sequence is then introduced. A description of uncertainties in engine selection follows. A discussion of model uncertainty concludes this section.

1. General Variables

Variables such as the moment of inertias, thruster misalignment angles, and engine moment arm, are assumed to be uncertain quantities. Table 3 lists these uncertainties and their representation in the analysis. For each variable, the probability distribution assumed and the corresponding parameters that define that probability distribution are provided. The various distributions listed in Table 3 were determined primarily by expert opinion (MER engineers and managers) and, to a lesser degree, statistical analysis.

2. Mission Sequence

The mission sequence provides a conduit to represent uncertainty in ACS operation. The nominal mission sequence involves de-spinning the spacecraft from 12 to 2 rpm shortly after separating from the launch vehicle's third stage. After several check out maneuvers, the primary objectives of the ACS are to perform slew maneuvers for communication and overcome the build-up of solar torque on the spacecraft. ACS must also be able to support fault protection (FP) in the event of any anomalies during cruise that might require ACS to autonomously slew to a sun-safe attitude or recovery from any undesirable attitude or rate changes. Uncertainties in the mission sequence are listed in Table 4. Uncertainties exist in when to perform slew maneuvers and in the magnitude of the actual slew.

3. Engine Selection

The MER project built on the organizational experience gained with the development and operation of MPF. The original design philosophy for ACS on MER was a replica ("build-to-print") of the 1996-1997 MPF design. The MER ACS design departed from the original MPF design due to lessons learned from MPF. Although there were changes to the original MPF flight software architecture and design as well as robustness additions for the cruise and entry, descent, and landing, the attitude control effectors (Aerojet MR-111C) remained unchanged from MPF. These existing engines were readily available (or easily procured) and assumed early in the MER ACS design instead of casting a wide net and looking at alternate engines. Hence, at the period around PDR there was no uncertainty in engine selection as the decision as to which engine type to use was made months earlier.

4. Model Uncertainty

The propellant mass model discussed in [10] is assumed to be itself uncertain. The uncertainty assumed for this model was assessed by expert opinion (MER engineers) to be normally distributed about zero with a standard deviation of 0.05 kg: $N(0, 0.05)$. Ideally the propellant mass model developed should be tested with several mission scenarios and compared to the actual propellant required for these missions. Unfortunately, there were no readily accessible examples available to test the model against. This is primarily because organizations involved in ACS operation

Table 4 Mission sequence uncertainties.

Mission sequence event	Time[a]	Maneuver type	Maneuver parameter	Distribution type and parameters	Units
De-spin from third stage	$C_d(1, 100\%)$	spin	ω_f	$N(2, 0.0667)$	rpm
Practice maneuver ("A practice")	$U_d(6, 10)$	slew[b]	ψ	$N(5, 0.5)$	deg
First-planned maneuver ("B1")	$U_d(15, 25)$	slew[b]	ψ	$N(50.45, 5)$	deg
Second-planned maneuver ("B2")	$U_d(40, 60)$	slew[b]	ψ	$N(5.13, 0.5)$	deg
Third-planned maneuver ("B3")	$U_d(75, 85)$	slew[b]	ψ	$N(6.35, 0.6)$	deg
Fourth-planned maneuver ("B4")	$U_d(90, 100)$	slew[b]	ψ	$N(2.76, 0.2)$	deg
Fifth-planned maneuver ("B5")	$U_d(110, 130)$	slew[b]	ψ	$N(8.51, 0.4)$	deg
Sixth-planned maneuver ("B6")	$U_d(135, 145)$	slew[b]	ψ	$N(9.88, 0.5)$	deg
Seventh-planned maneuver ("B7")	$U_d(155, 165)$	slew[b]	ψ	$N(5.64, 0.2)$	deg
Eighth-planned maneuver ("B8")	$U_d(166, 175)$	slew[b]	ψ	$N(5.04, 0.2)$	deg
Ninth-planned maneuver ("B9")	$U_d(176, 185)$	slew[b]	ψ	$N(5.75, 0.2)$	deg
Tenth-planned maneuver ("B10")	$U_d(186, 195)$	slew[b]	ψ	$N(4.47, 0.1)$	deg
Eleventh-planned maneuver ("B11")	$U_d(196, 205)$	slew[b]	ψ	$N(5.53, 0.1)$	deg
Twelfth-planned maneuver ("B12")	$U_d(206, 215)$	slew[b]	ψ	$N(5.85, 0.1)$	deg
FP: spin event	$C_d(216, 100\%)$	spin	ω_i	$\Gamma(11, 0.25)$	rpm
FP: spin recovery	$C_d(216, 100\%)$	spin	ω_f	$L(2, 0.0667)$	rpm
FP: emergency slew 1	$C_d(216, 100\%)$	slew[b]	ψ	$\Gamma(1.5, 10.5)$	deg
FP: emergency slew 2	$C_d(216, 100\%)$	slew[b]	ψ	$\Gamma(1.5, 10.5)$	deg
FP: emergency slew 3	$C_d(216, 100\%)$	slew[b]	ψ	$\Gamma(1.5, 10.5)$	deg
FP: emergency slew 4	$C_d(216, 100\%)$	slew[b]	ψ	$\Gamma(1.5, 10.5)$	deg
FP: emergency slew 5	$C_d(216, 100\%)$	slew[b]	ψ	$\Gamma(1.5, 10.5)$	deg
FP: emergency slew 6	$C_d(216, 100\%)$	slew[b]	ψ	$\Gamma(1.5, 10.5)$	deg

[a]days + launch; [b]no formal time requirement to complete slews within (30 minutes assumed); FP = fault protection

rarely keep detailed data in a format that could be incorporated or will not share this data for proprietary and/or International Traffic in Arms Regulations (ITAR) reasons. Model uncertainty is applied after MCS by convolving the model uncertainty distribution with the probabilistic results from simulation. In SS, model uncertainty is treated in analogous manner as a general input variable uncertainty.

E. Simulation and Analysis of Results

A deterministic case with input variables assuming their nominal values was first run to compare subsequent probabilistic results with. The results of this deterministic case indicated a total of 1.174 kg of propellant would be required by the attitude control system. This 1.174 kg comprises 0.301 kg for spin maneuvers, 0.137 kg for slew maneuvers, 0.200 kg for solar torque compensation, and 0.536 kg for fault protection. For the two simulation techniques, the number of calls to the propellant mass required model was set at $N_T = 10{,}000$ for MCS and $N = 500$ for SS (per SS level). Subset Simulation is implemented with parameters $p_0 = 0.1$ and $\chi = 1$. Four simulation levels (0 to 3), each with 500 samples, are carried out so that the smallest tail probability that can be covered is of the order of 10^{-4}. In other words, confidence limits up to 99.99% are covered.

All subsequent tables and figures reflect the final uncertainty in propellant mass required. The CDF values for both MCS and SS are shown in Fig. 4.

Figures 4(b) to (d) demonstrate the performance of both simulation techniques at the upper tail of the distribution. Monte Carlo simulation is the benchmark for comparison but requires a substantial number of calls to the model (N_T) to obtain values for the entire CDF range. As theorized, SS provides a comparable accuracy as MCS at the CDF tail despite requiring only a fifth the calls to the model. Table 5 details the statistics of SS by simulation level for propellant mass.

The low values of γ in Table 5 indicate that the modified MCMC algorithm is accepting new samples at each simulation level within a chain. This is evident from Eq. (7), because when a new sample is rejected the next sample on the Markov Chain is taken as the current sample. If this happens frequently it will significantly increase

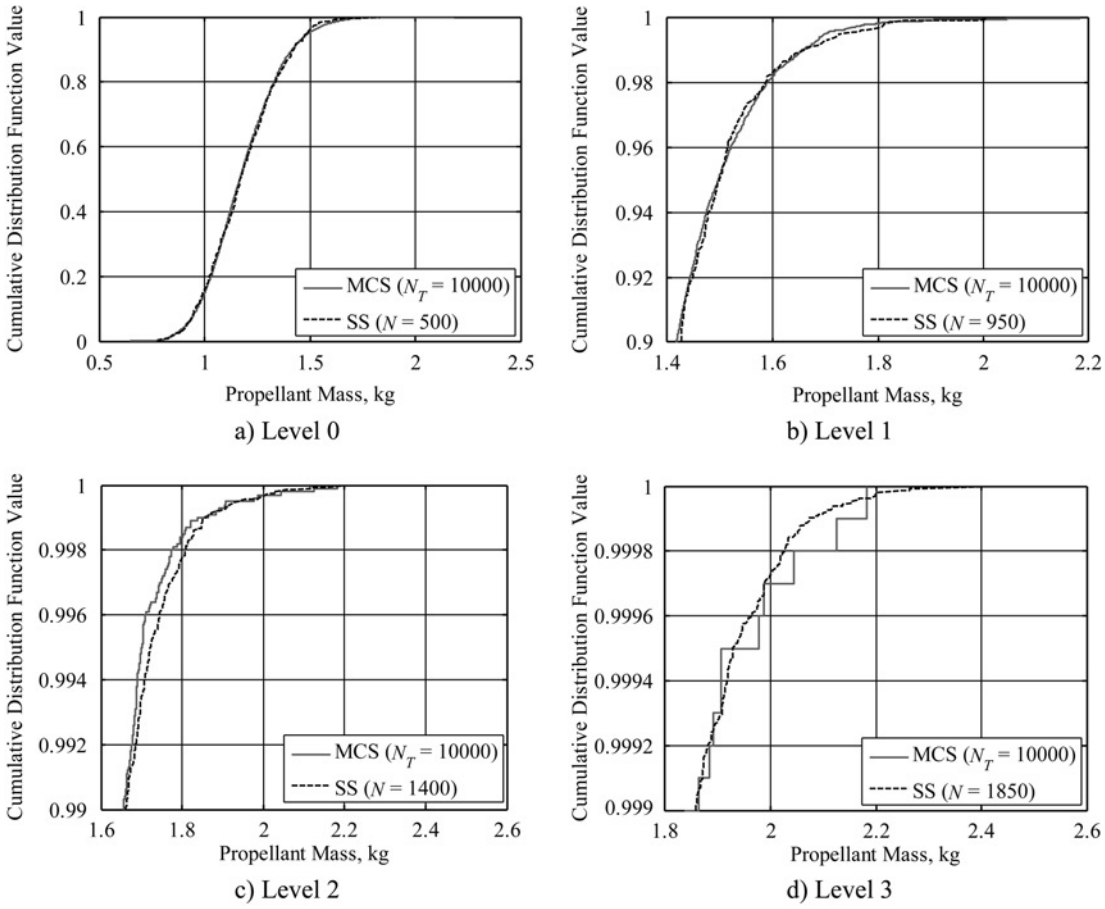

Fig. 4 Propellant mass CDFs at different simulation levels.

the correlation among samples and hence γ. The choice of $\chi = 1$ provided a reasonably low-value of γ yielding satisfactory efficiency. Alternate values of χ were not exhaustively investigated to optimize the efficiency. It should be noted from Table 5 that there is significant discrepancy between SS and MCS results at simulation level 3 (which would be of interest to an extremely risk-averse decision maker). This is partially due to estimation error in MCS as the final column indicates SS achieves a comparable accuracy as 70,779 MCS samples (N_{MCS}) whereas only $N_T = 10{,}000$ were performed for MCS. The error drops to +0.40% when compared to 70,000 MCS samples. Hence, SS provides comparable results as Monte Carlo at this 99.99$^{\text{th}}$ percentile value yet requires only a fraction (1,850/70,000 $\approx$ 2.6%) of the number of samples.

Table 5 SS results by level.

SS Level	N_{SS}	x	P_x(kg)	$P^{\text{a}}_{\text{MCS}}$ (kg)	Error[b] (%)	γ	δ	N_{MCS}
0	500	90	1.426	1.417	+0.61	0	0.13416	500
1	950	99	1.660	1.655	+0.31	0.91	0.22894	1,889
2	1,400	99.9	1.858	1.851	+0.40	1.06	0.29905	11,171
3	1,850	99.99	2.074	2.154	−3.75[c]	1.88	0.37586	70,779

[a]MCS results using 10,000 samples; [b]relative to the 10,000 MCS samples; [c]MCS is not accurate at this extreme tail value of x

Comparing the values provided in Table 5 indicate that SS provides comparable estimates of the propellant mass required at the percentiles of interest at a fraction of the samples. Comparing the results in Table 5 with the MER project propellant mass estimate of 4.4 kg and the actual mission values of 0.646 kg (for MER-A) and 0.738 kg (for MER-B) indicate both the current worst-case deterministic approach and the proposed method are conservative. It seems the uncertainties assumed in estimating the propellant mass were either overestimated or the propellant mass came in extremely low. If the uncertainties were overestimated (as is more likely), the proposed approach can be revised in subsequent implementations (on future missions) taking into account the actual mission results from MER-A and MER-B and higher-fidelity propellant-mass model. Although the overall cost of implementing the proposed approach, whether by MCS or SS, is small in the overall design of a spacecraft attitude control system, arguably its greatest benefit is improved decision making. The proposed approach provides a more rigorous, transparent, repeatable, and tenable method that the current worst-case deterministic method fails to provide.

Figure 5 shows the conditional samples at different simulation levels of four selected input variables: the moment of inertia about the spin axis (J_{zz}), the distance between the center of pressure and the center of mass (κ), the third emergency slew angle (ψ_3), and the modeling error (X). Level 0 corresponds to direct MCS, where the samples are generated from their original PDF. The histograms that correspond to the original PDF of each variable are shown with dashed lines. For each variable θ, for example, the difference between the conditional histogram and its original distribution is an indication of its 'sensitivity', interpreted here as the variation of $P(Y > y|\theta)$ with θ, because $P(Y > y|\theta) = P(Y > y)p(\theta|Y > y)/p(\theta)$. In particular, when the conditional histogram is identical to the original distribution, it shows that the particular variable does not influence the response Y.

From Fig. 5, it is interesting to note that the conditional histogram of J_{zz} shifts to the right at level 1 as the simulation level increases, showing that high values of propellant mass are probabilistically associated with high values of J_{zz}. Further investigation reveals no significant change in the histograms of J_{xx} and J_{yy} (not shown here) from their original distribution, even though the source uncertainty associated with J_{xx} and J_{yy} implies a greater COV than that of J_{zz} (see Table 3). Thus, in order to reduce the uncertainty in the propellant mass, it is more

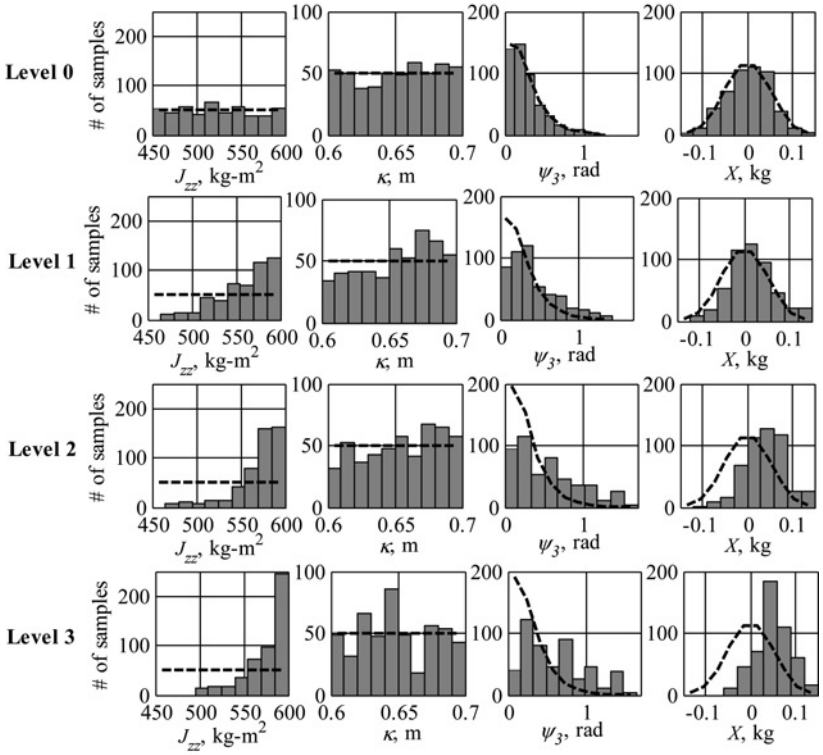

Fig. 5 Conditional samples for four variables at each simulation level.

effective to mitigate the uncertainty of J_{zz} than J_{xx} or J_{yy}. The variables κ and ψ_3 do not show significant change in their conditional histogram, although a slight shift to the left is observed for ψ_3 at level 1 and above. There is a graduate but slight shift in the histogram of the modeling error X as the simulation level increases, as expected. Investigation of the conditional histogram of other input variables show that many do not differ significantly from the original distribution, even at high-simulation levels that correspond to high values of propellant mass. This indicates that tail probability of the propellant mass is not necessarily due to the probabilistic occurrence of some variables appearing at the tail, but as a result of their collective arrangement. Similar phenomenon has been observed in the study of dynamical systems subjected to stochastic excitations, where it was found that excessive response was due to resonance in the frequency content of the excitation with the natural frequency of the system.[24] Finally, it should be noted that a similar investigation of the conditional histograms could have been carried out using direct MCS, but it would have required significantly more computational effort than SS. For example, to obtain one conditional sample at Level 3 (99.9^{th} percentile), requires on average 1,000 samples, i.e., system analyses. Thus, to obtain 500 conditional samples for constructing the histograms as shown in the last row of Fig. 5, requires on average 500,000 samples, which demands significantly more computational effort than SS (that requires only 1,850 samples).

IV. Conclusion

A method for quantifying uncertainty in conceptual-level design via Subset Simulation is described. As an example application, the investigated method is applied to estimating the propellant mass required by a spacecraft to perform attitude control. Subset Simulation is modified to account for differences between the aerospace engineering application and the original structural-analysis application the algorithm was originally developed for. The results of Subset Simulation are compared with traditional Monte Carlo simulation. The investigated method allows uncertainty in the propellant mass required to be quantified based on the risk tolerance of the decision maker. For the attitude control example presented, Subset Simulation successfully replicated Monte Carlo simulation results yet required significantly less computational effort. In the case of an extremely risk-averse decision maker, Subset Simulation achieved comparable results to Monte Carlo simulation while requiring less than three percent of the computational expense.

Acknowledgments

The authors thank Milos Ilak (formerly of Swarthmore College, Swarthmore, PA; now at Princeton University, Princeton, NJ) who developed the original propellant mass model discussed. The authors also thank Steve Collins and Miguel San Martin (Mars Exploration Rover Project, JPL, Pasadena, CA). This research was funded in part by the Space Systems, Policy, and Architecture Research Consortium (SSPARC), a joint research program funded by the U.S. government involving the Massachusetts Institute of Technology, Caltech, and Stanford University, and subsequently by the Singapore Ministry of Education (MoE) through research grant ARC8/05. Part of the research was carried out at Caltech with the documentation accomplished by the authors at Nanyang Technological University and City University of Hong Kong. The MER attitude determination and control design effort was carried out by JPL, California Institute of Technology under a contract with the National Aeronautics and Space Administration.

References

[1]Thunnissen, D., "Uncertainty Classification for the Design and Development of Complex Systems," *Proceedings of the* 3^{rd} *Annual Predictive Methods Conference*, Veros Software, Santa Ana, CA, June 2003.

[2]Siddall, J., *Probabilistic Engineering Design: Principles and Applications*, Marcel Dekker, Inc., New York, NY, 1983.

[3]Cox, R., *The Algebra of Probable Inference*, John Hopkins Press, Baltimore, MD, 1961.

[4]Papoulis, A., *Probability, Random Variables, and Stochastic Processes*, McGraw-Hill, Inc., New York, NY, 1965.

[5]Jaynes, E., and Jaynes, E.T., *Papers on Probability, Statistics, and Statistical Physics*, Kluwer Academic Publishers, Dordrecht, Holland, 1989.

[6]Pradlwarter, H., Pellissetti, M., Schenk, C., Schuëller, G., Kreis, A., Fransen, S., Calvi, A., and Klein, M., "Realistic and Efficient Reliability Estimation for Aerospace Structures," *Computer Methods in Applied Mechanics and Engineering*, Vol. 194, No. 12–16, 8 April 2005, pp. 1597–1617.

[7]Pellissetti, M., Schuëller, G., Pradlwarter, H., Calvi, A., Fransen, S., and Klein, M., "Reliability Analysis of Spacecraft Structures under Static and Dynamic Loading," *Computer and Structures*, Vol. 84, No. 21, August 2006, pp. 1313–1325.

[8]Au, S.K., "On the Solution of First Excursion Problems by Simulation with Applications to Probabilistic Seismic Performance Assessment," PhD thesis, California Institute of Technology, Pasadena, CA, 2001.

[9]Au, S.K., and Beck, J., "Estimation of Small Failure Probabilities in High Dimensions by Subset Simulation," *Probabilistic Engineering Mechanics*, Vol. 16, No. 4, 2001, pp. 263–277.

[10]Thunnissen, D., "Propagating and Mitigating Uncertainty in the Design of Complex Multidisciplinary Systems," PhD thesis, California Institute of Technology, Pasadena, CA, 2005.

[11]Thunnissen, D., Au, S.K., and Tsuyuki, G., "Uncertainty Quantification in Estimating Critical Spacecraft Component Temperatures," *Journal of Thermophysics and Heat Transfer*, Vol. 21, No. 2, April–June, pp. 422–430.

[12]Roberts, C. and Casella, G., *Monte Carlo Statistical Methods*, Springer, New York, NY, 1999.

[13]Metropolis, N., Rosenbluth, A., Rosenbluth, M., and Teller, A., "Equations of State Calculations by Fast Computing Machines," *Journal of Chemical Physics*, Vol. 21, No. 6, 1953, pp. 1087–1092.

[14]Hastings, W., "Monte Carlo Sampling Methods Using Markov Chains and their Applications," *Biometrika*, Vol. 57, No. 1, 1970, pp. 97–109.

[15]Au, S.K., Ching, J., and Beck, J., "Application of Subset Simulation Methods to Reliability Benchmark Problems," *Structural Safety*, Vol. 29, No. 3, July 2007, pp. 183–193.

[16]Schuëller, G., and Pradlwarter, H., "Benchmark Study on Reliability Estimation in Higher Dimensions of Structural Systems," *Structural Safety*, Vol. 29, No. 3, July 2007, pp. 167–182.

[17]Roncoli, R., and Ludwinski, J., "Mission Design Overview for the Mars Exploration Rover Mission," Paper AIAA 2002-4823, August 2002.

[18]D'Amario, L., "Mars Exploration Rover (MER) Project Navigation Plan," Jet Propulsion Laboratory, D-19660, California Institute of Technology, Pasadena, CA, 4-60, 2002.

[19]Kaplan, M., "Momentum Precession and Adjustment for a Rigid Spacecraft," *Modern Spacecraft Dynamics and Control*, John Wiley & Sons, New York, NY, pp. 124–127.

[20]Chobotov, V., "Vehicle Reorientation in Space," *Spacecraft Attitude Dynamics and Control*, Krieger Publishing Company, Malabar, FL, pp. 22–23.

[21]Ganapathi, G., Birur, G., Tsuyuki, G., McGrath, P., and Patzold, J., "Active Heat Rejection System on Mars Exploration Rover—Design Changes from Mars Pathfinder," *Proceedings of the Space Technology and Applications International Forum (STAIF)*, Institute for Space and Nuclear Power Studies, Albuquerque, NM, 2003, pp. 206–217.

[22]Thunnissen, D., "Method for Determining Margins in Conceptual Design," *Journal of Spacecraft & Rockets*, Vol. 41, No. 1, January–February 2004, pp. 85–92.

[23]Thunnissen, D., and Tsuyuki, G., "Margin Determination in the Design and Development of a Thermal Control System," *SAE 2004 Transactions: Journal of Aerospace*, Vol. 113, No. 1, 2005, pp. 899–916.

[24]Au, S.K., and Beck, J., "Subset Simulation and its Applications to Seismic Risk Based on Dynamic Analysis," *Journal of Engineering Mechanics*, Vol. 129, No. 8, 2003, pp. 1–17.

Christopher Rouff
Associate Editor